Biochimica et Biophysica Acta 812 (1985) 609–623
Elsevier

BBA 72421

Structure-function studies of canine cardiac sarcolemmal membranes. II. Structural organization of the sarcolemmal membrane as determined by electron microscopy and lamellar X-ray diffraction

L.G. Herbette [a,b,*], T. MacAlister [c], T.F. Ashavaid [a] and R.A. Colvin [a]

Departments of Medicine [a], Biochemistry [b] and Microbiology [c], University of Connecticut Health Center, Farmington, CT 06032 (U.S.A.)

(Received July 6th, 1984)

Key words: Membrane morphology; Sarcolemmal membrane; Freeze-fracture; X-ray diffraction; (Canine heart)

The morphological and ultrastructural properties of highly purified canine cardiac sarcolemmal vesicles, prepared by a modification (Colvin, R.A., Ashavaid, T.F. and Herbette, L.G. (1985) Biochim. Biophys. Acta 812, 601–608) of the method of Jones et al. (Jones L.R., Madlock, S.W. and Besch, H.R. (1980) J. Biol. Chem. 255, 9971–9980), were examined by several techniques. Thin-section electron microscopy showed predominantly intact unilamellar vesicles with little staining beyond the lipid bilayer boundaries. Freeze-fracture electron microscopy demonstrated that the majority of particles are approx. 90 Å diameter and present at a density of 780 ± 190 μm^{-2} ($\pm$S.D.). If it is assumed that some of these particles represent the $(Na^+ + K^+)$-ATPase, the finding that they are largely confined to the convex fracture face suggests a predominant right-side-out orientation of these sarcolemmal vesicles that is consistent with biochemical assays. The sarcolemmal membrane width measured by electron microscopy (unhydrated membrane width of 50–70 Å) is consistent with the unit cell dimensions of 56–77 Å determined by lamellar X-ray diffraction (hydrated membrane width). A unit cell dimension of 56–62 Å was also found by X-ray diffraction for sarcolemmal lipids extracted from these preparations, indicating that the isolated sarcolemmal preparations do not contain a significant surface coat (glycocalyx). As both cardiac and skeletal sarcoplasmic reticulum membranes have a 80–100 Å membrane width, these findings demonstrate that the purified sarcolemmal membrane is structurally distinct from both cardiac and skeletal sarcoplasmic reticulum. In contrast to the protein-rich skeletal sarcoplasmic reticulum membrane, which contains a single essential protein responsible for the regulation of cytosolic Ca^{2+} concentration, the sarcolemma is a lipid-rich membrane that contains a variety of proteins associated with many regulatory functions served by this membrane in cardiac muscle.

Introduction

The sarcolemmal and sarcoplasmic reticulum membranes play a central role in the regulation of myocardial function. Of these two membranes, the sarcoplasmic reticulum is far simpler from a functional standpoint as this internal membrane is involved primarily, if not exclusively, with the regulation of cytosolic calcium concentration [3,4] and its functional expression in the processes of excitation-contraction coupling. This highly specialized membrane contains a single essential protein, the Ca^{2+} pump ATPase, which carries out a limited number of well-defined functions related to Ca^{2+} transport. During the past decade, the enzymatic mechanism responsible for active

* To whom correspondence should be addressed.

calcium transport by the sarcoplasmic reticulum has been characterized [5] and a structural picture of this membrane system has been developed from ultrastructural electron microscope images and X-ray and neutron diffraction studies [6–20].

In contrast to the sarcoplasmic reticulum, the sarcolemma has a much more complex role in cellular function, being involved in virtually all communication between the cell interior and the extracellular space. The sarcolemmal membrane might therefore be expected to contain a number of different proteins and to have a different structural organization from that of the sarcoplasmic reticulum. The present report describes our initial characterization of the structural properties of cardiac sarcolemmal membranes purified according to the procedure by Jones et al. [2]. This membrane was found to be structurally distinct from that of both purified cardiac and skeletal sarcoplasmic reticulum. Our determination of the sarcolemmal membrane architecture suggests that receptor sites may reside at the surface or within the lipid bilayer of the sarcolemmal membrane, but does not exclude the possibility of undetected protein receptors at low concentrations protruding from either surface of the sarcolemmal membrane, since drug-receptor binding site densities were found to be quite low [1]. The most distinct physical property of the sarcolemmal membrane is a lipid/protein ratio that is much higher than that of skeletal and cardiac sarcoplasmic reticulum [1] and this finding may be important in understanding how lipophilic substances interact with sarcolemmal membrane receptors.

Methods

Canine sarcolemmal and sarcoplasmic reticulum membrane preparations

Sarcolemmal vesicles were purified by a modification [1] of the method of Jones et al. [2]. All sarcolemmal vesicle dispersions were kept on ice and used within one day of preparation for electron microscopy and X-ray diffraction studies. Cardiac sarcoplasmic reticulum vesicles, isolated from canine ventricular myocardium [21], were prepared by the method of Katz et al. [22] and purified further by zonal centrifugation in a discontinuous sucrose gradient [23]. Sarcoplasmic reticulum vesicles were prepared from rabbit white skeletal muscle by the method of Katz et al. [22]. A 'light' fraction, enriched in longitudinal sarcoplasmic reticulum membranes [24] and referred to as sarcoplasmic reticulum was used in all experiments described in this report. Cardiac and skeletal sarcoplasmic reticulum membrane dispersions in approx. 30% sucrose were quick frozen in liquid nitrogen, stored at −90°C, thawed and used for experiments within 2–3 weeks of initial preparation. Protein concentrations were determined by the method of Lowry et al. [25].

Electron microscopy

Thin-section dispersions. Freshly prepared sarcolemmal, skeletal and cardiac sarcoplasmic reticulum vesicles were resuspended in 150 mM NaCl/5 mM Tris (pH 7.2) and pelleted by centrifugation at $g_{av} = 81\,000$ for 60 min in an SW-27 swinging bucket rotor, the resulting pellets overlayed with 1% tannic acid and 4% glutaraldehyde in 100 mM sodium cacodylate buffer (pH 7.2) [15], and fixed for 2 h at 4°C. The fixed pellets were washed extensively with 100 mM cacodylate buffer, fixed with 2% OsO_4 in cacodylate buffer for 1.5 h, then washed briefly with water and incubated with 1% aqueous uranyl acetate at 60°C for 30 min. After dehydration with ethanol, the pellets were embedded in Polybed 812. Thin sections were cut with a diamond knife on an MT2-B ultramicrotome, mounted on copper grids, and counterstained with uranyl acetate and lead citrate. The sections were examined with a Hitachi Hu 11-E electron microscope (Hitachi, Ltd., Tokyo, Japan) at an accelerating voltage of 75 kV [14].

Freeze-fracture dispersions. Sarcolemmal or skeletal sarcoplasmic reticulum membrane vesicles were resuspended in 150 mM NaCl/5 mM Tris (pH 7.2), pelleted as described above for thin-section preparations, and overlayed with 20% glycerol for 2 h at 4°C. Specimens were mounted on gold discs and frozen in a Freon slush cooled by liquid nitrogen. Specimens were freeze-fractured at −100°C and deep-etched at −100°C on a Balzers B360M freeze-etching apparatus (Balzers High Vacuum Corp., Santa Anna, CA). Specimens received a 6 s application of platinum and carbon being unidirectionally shadowed at an angle of 50° producing shadow thicknesses of approx. 100 and

approx. 200 Å, respectively. This relatively high shadow angle was chosen to reduce the degree of shadow cast in our micrographs. The replicas were floated off onto distilled water, cleaned with 5% Clorox, and picked up on electron microscope grids. Grids were examined in a Hitachi Hu 11-E electron microscope (Hitachi, Ltd., Tokyo, Japan) with an accelerating voltage of 75 kV. Freeze-etching was performed on samples in the absence of glycerol in order to determine the origin of the fracture planes for sarcolemmal vesicles.

The density of particles in the freeze-fracture plane was determined by using stereological method III as described by Napolitano et al. [14]. A test circle was placed on a convex profile for which the radius of the test circle was appropriately matched to the radius of the convex profile so as to avoid spatial distortions of the particle distribution near the edges of the freeze-fracture profile. Particle densities were determined based on the number of particles with 50% or more of their area within the test circle. Approx. 100 vesicles of varying size were selected from several different sarcolemma preparations and averaged to provide a representative particle density for these preparations. Napolitano et al. [14] have shown that the particle densities obtained using this method are similar to the results obtained using a small fixed test circle randomly placed a number of times on the freeze-fracture profile. These procedures tend to reduce the errors in determining particle densities which arise from visualizing particles in the freeze-fracture profile as a function of the angle subtended by the shadow cast.

Thin-section membrane multilayers. Hydrated oriented multilayers composed of sarcolemmal membranes (100–200 μg protein) were prepared as previously described for skeletal sarcoplasmic reticulum membranes [11] in 150 mM NaCl/5 mM Tris (pH 7.2). After these membrane multilayers were partially dehydrated at 88% relative humidity at 5°C for approx. 20 h, a vial of 4% osmium was placed in the relative humidity chamber and the membrane multilayer allowed to fix via the vapor phase for several hours [15]. These fixed multilayers were then simultaneously counter-stained with 1% uranyl acetate and dehydrated, and then embedded as described previously [15]. Thin sections were cut approximately parallel to the sedimentation axis of the multilayer. Well-defined regions in these electron micrograph negatives which depicted the multilayer structure were masked-off and mounted in an optical diffractometer with the plane of the electron micrograph perpendicular to the laser beam [14]. Optical diffraction patterns of these regions were obtained as previously described [14] to determine the average unit cell repeat of the multilayer.

Freeze-fracture membrane multilayers. Hydrated oriented multilayers composed of sarcolemmal membranes (approx. 400 μg protein) were prepared as described above, by centrifugation onto clear plastic discs. These samples were partially dehydrated at 88% relative humidity. The sample was quick frozen by placing a precooled (Freon slush cooled by liquid nitrogen) brass cylinder on top of the multilayer sample. The clear plastic disc/ sample/ brass cylinder sandwich was mounted on a Balzers B360M freeze-etching apparatus. The sample was fractured by quickly removing the brass cylinder and the fractured surface was prepared as described above for dispersions. This procedure provided a fracture profile of the sarcolemmal membrane which was, on average, perpendicular to the sedimentation axis of the multilayer sample, i.e., corresponding to the plane of the membrane normal to the bilayer axis.

Lamellar X-ray diffraction

Hydrated oriented multilayers of sarcolemmal membranes at a concentration of approx. 0.05 mg protein/ml were formed on aluminum foil substrates by centrifugation in 150 mM NaCl/5 mM Tris (pH 7.2) using a special apparatus as described [11]. Lipids were extracted from sarcolemmal membranes [1] and evaporated to dryness under argon. The same buffer medium used to resuspend sarcolemmal vesicles (150 mM NaCl/5 mM Tris (pH 7.2)) was added to the dried lipid sample to give a final concentration of 0.05 mg lipid/ml and the sample was vortexed for 1–3 min. The resulting liposomal dispersion was centrifuged as described [11]. Both intact sarcolemmal membrane and sarcolemmal lipid multilayers usually contained about 300 nmol phosphate. The membrane multilayers on foil were glued to curved glass slides [11] and placed over

one of several saturated salt solutions defining a relative humidity range of 45–90%. These unfixed oriented membrane multilayers were exposed to a collimated, monochromatic X-ray beam (CuK_α X-rays, $\lambda = 1.54$ Å, $K_\alpha 1$ and $K_\alpha 2$ being unresolved) from a Rigaku-Denki RU3 rotating anode generator using a Searle diffraction camera (Baird and Tatlock, Ltd., Essex, U.K.) with one vertical Franks' mirror. The curved multilayer specimen (temperature and relative humidity regulated, 5–10°C, 45–90% relative humidity) was oriented with respect to the X-ray beam at near grazing incidence in order to obtain the lamellar meridional diffraction pattern, which was recorded on X-ray-sensitive film (Kodak no screen type NS5T).

The lamellar diffraction patterns recorded on film were traced on a Helena Laboratories Quick Scan R & D densitometer modified to scan slowly through the center of each reflection arc along the lamellar meridional axis of the film with a 10 μm wide slit image. The integrating slit beam height was made considerably smaller than the height of the full extent of the lamellar reflections. The intensity data ($I(s)$) were transferred directly to computer memory, and a background curve generated by a spline-fit algorithm [26,27] was subtracted digitally from the total intensity function providing a background-corrected intensity function, $I_c(s)$. These lamellar reflections were integrated using a Gaussian fitting routine. Lamellar intensity functions from sarcolemmal membranes were corrected by a factor of $s^2 = (2\sin\theta/\lambda)^2$, since the inherent mosaic spread of the lamellar diffraction was considerably larger than the height of the integrating slit used (see Fig. 4B and C). The lamellar intensity functions of lipids extracted from the sarcolemmal membrane were corrected by one factor of s, since the inherent mosaic spread was considerably smaller (see Fig. 4A) resulting in a more uniform intensity distribution along the lamellar reflection in a direction perpendicular to the lamellar meridional axis. The origin of these correction factors has been previously discussed [11,15,17,28]. Unit cell dimensions (d) were obtained from the spacing of these lamellar reflections. The lamellar intensities were phased by the swelling method [29] using a previously described algorithm [30]. The corrected and properly phased structure factors, $F(h)$, where h is the diffraction order index, were used in a Fourier series according to Guinier [31]:

$$\rho(x) = \frac{2}{d} \sum_{h=1}^{h\max} F(h)\cos(2\pi hx/d)$$

to provide the corresponding electron density profile structures at approx. 15 Å resolution.

Materials

All chemicals used were reagent grade. Deionized water was glass-distilled prior to use.

Results

Electron microscopy

Thin-section profiles of typical sarcolemmal vesicle dispersions illustrated in Fig. 1A show their vesicular nature and variable vesicle size. Thin-section micrographs from several preparations showed a predominant population of unilamellar vesicles with an occasional multilamellar structure appearing in the micrograph field. In contrast to thin-sectioned skeletal (Fig. 1B) and cardiac (data not shown) sarcoplasmic reticulum membrane vesicles, thin-sectioned sarcolemmal vesicles lacked extensive tannic acid staining on either membrane surface. This finding suggests that the sarcolemmal membrane contains few detectable protein protrusions beyond the limits of the sarcolemmal lipid bilayer. Other staining methods (i.e., ruthenium red, osmium-thiocarbohydrazide-osmium, and negative staining) also failed to show significant staining at either face of the sarcolemmal membrane (data not shown), whereas cardiac and skeletal sarcoplasmic reticulum membranes treated in a similar manner showed substantial staining at the extravesicular surface of the vesicles.

The thickness of a single sarcolemmal membrane determined from thin sections of vesicle dispersions (Fig. 1A) was approx. 50–70 Å. Thin-sectioned osmium-fixed multilayers of sarcolemmal membranes gave the appearence of a symmetrically stained banding pattern (Fig. 2A). The micrograph shown in Fig. 2 is representative of both many different fields within the same thin section and of many different sarcolemmal preparations. A regular repeat spacing of 30–40 Å was measured by optical diffraction of these elec-

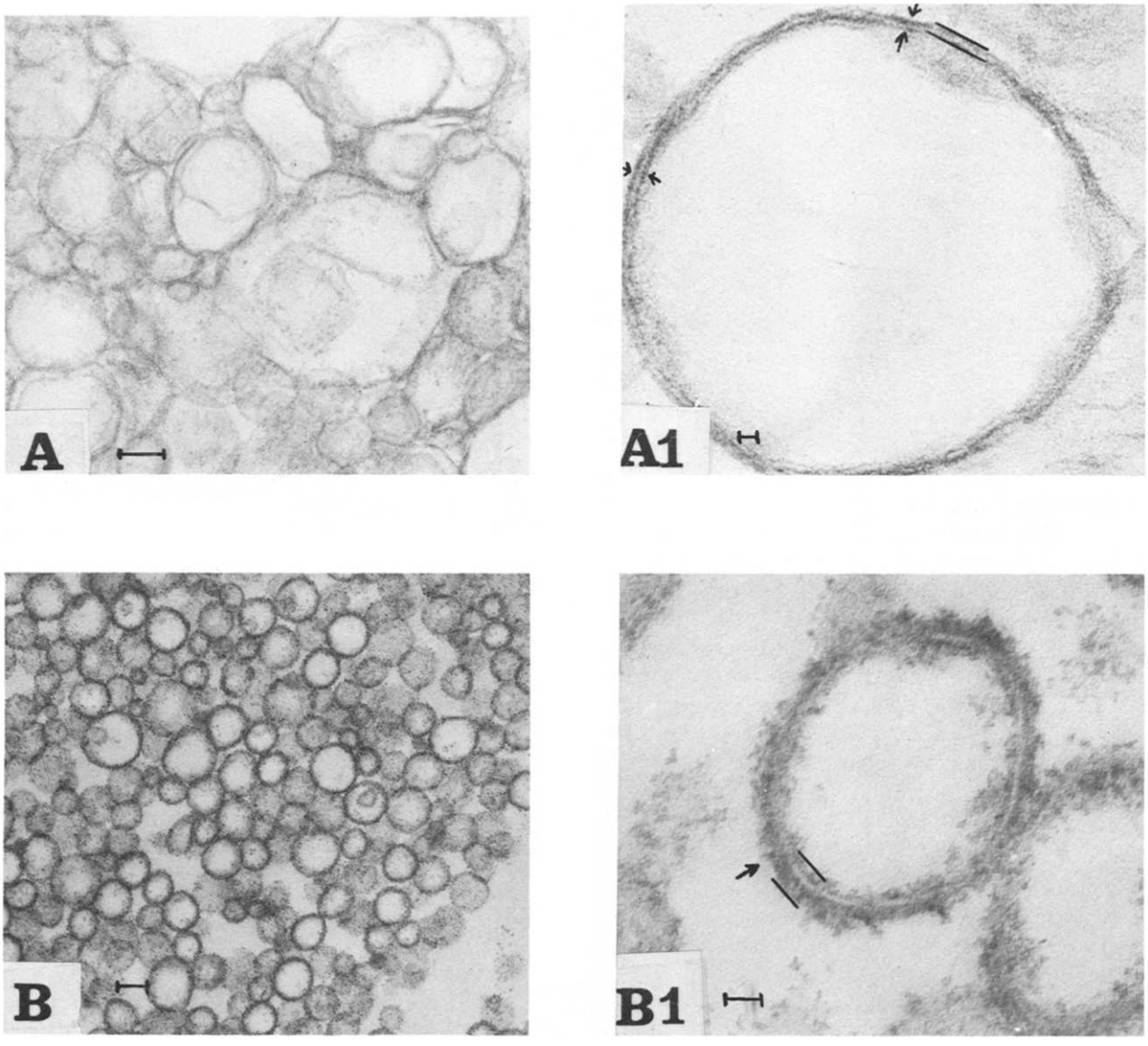

Fig. 1. Thin section (tannic acid-osmium) of sarcolemmal vesicles (A) and skeletal sarcoplasmic reticulum vesicles (B). The arrows in (A1) point to the lack of tannic acid-mediated staining at either surface of the sarcolemmal membrane contrasted to the arrow in (B1) showing substantial staining at the extravesicular surface of the sarcoplasmic reticulum membrane. The bar for the low-magnification fields equals 0.1 μm; the bar for the high-magnification fields equals 0.01 μm.

tron micrograph negatives (Fig. 2B). This repeat corresponds to the average center-to-center distance of the electron opaque bands seen in the electron microscope, and represents the minimum thickness of a single, unhydrated symmetrically staining sarcolemmal membrane in a compressed multilayer (compare Figs. 1A and 2A). No other repeat spacings could be qualitatively observed or quantitatively measured. Thin sections of skeletal sarcoplasmic reticulum dispersions show a much greater membrane width of approx. 90–100 Å (Fig. 1B), and thin-sectioned osmium-fixed membrane multilayers of skeletal sarcoplasmic reticulum have a repeat distance of 180 Å which has been shown to represent a unit cell composed of the two asymmetric membranes of the flattened

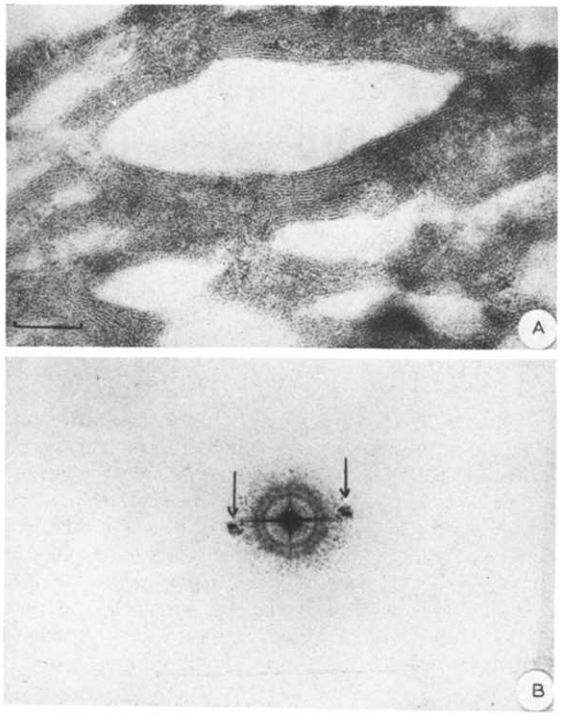

Fig. 2. Thin section (A) of osmium vapor fixed multilayers of sarcolemmal membrane. The micrograph shows stacks of flattened membranes with an average repeat of 30 Å as calculated from the position of the first order (arrows) of the optical diffraction pattern shown in (B). Bar equals 0.05 μm.

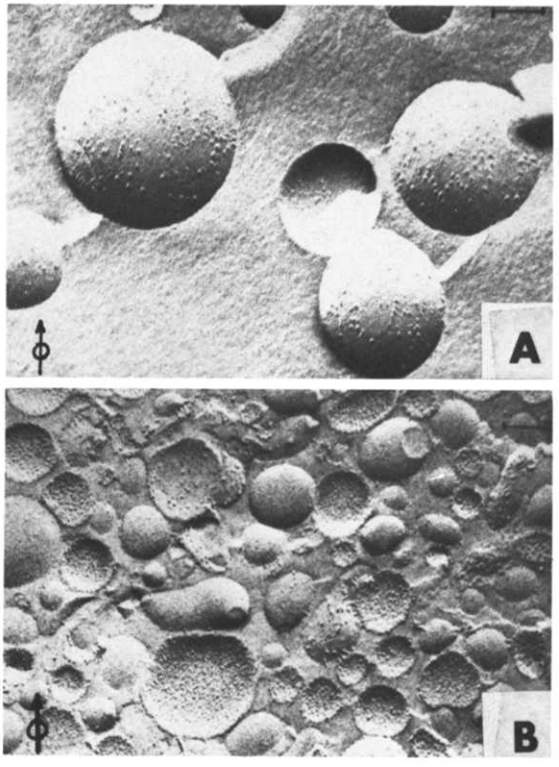

Fig. 3. In (A), typical freeze fracture of the majority of our sarcolemmal preparations showing large particles predominantly localized on the convex fracture face. The fracture plane is at the center of the sarcolemmal lipid bilayer as determined by freeze-etching (see text). In (B), freeze fracture of skeletal sarcoplasmic reticulum with particles primarily on the concave fracture surface. Bar equals 0.1 μm.

sarcoplasmic reticulum vesicle in the oriented multilayer [15]. For this case, the unhydrated asymmetric average membrane width in the sarcoplasmic reticulum multilayer is thus approx. 90 Å, which is consistent with measurements of thin-sectioned sarcoplasmic reticulum dispersions. Estimates of membrane widths for sarcolemma derived from either dispersions or membrane multilayers are therefore consistent and differ significantly from estimates of sarcoplasmic reticulum membrane widths also derived from either dispersions or multilayers.

Close inspection of the fracture surfaces formed by freeze-etching showed that the sarcolemmal membrane vesicle had fractured along a plane coincident with the center of the lipid bilayer, yielding an outer concave and an inner convex fracture surface (data not shown). Freeze-fracture profiles of all sarcolemmal vesicle preparations (Fig. 3A) showed large (90 ± 10 Å diameter) particles predominantly on the convex fracture surfaces. These large particles on the sarcolemmal fracture surface appeared in a ratio of approx. $85/15 \pm 5\%$ on the convex vs. concave fracture surfaces. In contrast, freeze-fracture profiles of skeletal sarcoplasmic reticulum had smooth convex fracture surfaces and concave fracture surfaces that were uniformly studded with homogeneous (80 ± 10Å diameter) particles (Fig. 3B) as previously described [14].

The large particles on the sarcolemmal convex fracture surface were similar in size to those observed for the concave fracture surface of sarcoplasmic reticulum. However, utilizing stereological methods [14], the density of these particles for all

sarcolemmal preparations was much lower: 780 ± 190 μm^{-2} ($n = 102$, ± S.D.) in contrast to sarcoplasmic reticulum which is 11 500 ± 2000 μm^{-2} ($n = 100$, ± S.D.) [14].

Freeze fracture of sarcolemmal membrane multilayers showed that these large particles were randomly distributed within the plane of the sarcolemmal membrane. If the distribution of these large particles is representative of other protein constituents in the sarcolemmal membrane, this observation supports the view that there is negligible in-plane aggregation of protein in the sarcolemmal membrane multilayer. Thus, multilayer samples used for X-ray diffraction studies do not contain lateral phase segregated protein.

Lamellar X-ray diffraction of sarcolemmal membranes

Thin sections of sarcolemmal vesicle dispersions (Fig. 1) and the functional sidedness assays described in the accompanying paper [1] demonstrate that the multilayer samples used for diffraction studies are formed from predominantly unilamellar vesicles with a high degree of sidedness. This sidedness is preserved following centrifugation prior to the dehydration step to orient the multilayer and thus the multilayer unit cell would contain a center of symmetry as for the sarcoplasmic reticulum membrane [11,15]. Lamellar meridional X-ray diffraction data, obtained from these hydrated unfixed multilayers of sarcolemmal membranes, showed that sarcolemmal membranes can orient under conditions similar to those used for sarcoplasmic reticulum membranes [11]. Lamellar diffraction data for sarcolemmal membranes yielded average multilayer unit cell repeat distances, d, between 56 and 77 Å, depending on the water content of the multilayer. Lamellar diffraction data for extracted sarcolemmal lipids yielded unit cell repeat distances between 56 and 62 Å. Diffraction patterns within these unit cell ranges for extracted lipids and the sarcolemmal membrane (Fig. 4) and patterns measured by densitometry (Fig. 5) have characteristically different mosaic spreads and reflection widths. It was found that the diffraction patterns for extracted lipids exhibited a significantly less degree of mosaic spread compared to the diffraction patterns of sarcolemmal membranes. In addition, the full

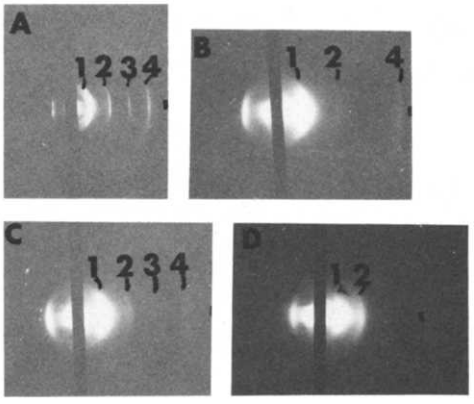

Fig. 4. (A) Lamellar meridional X-ray diffraction pattern of lipids extracted from the sarcolemmal membrane indexing on an average repeat of 60 Å. Lamellar meridional X-ray diffraction patterns of the sarcolemmal membrane indexing on an average repeat of 56 Å (B), 63 Å (C) and 77 Å (D). The first order, $I(h = 1)$, of these diffraction patterns are overexposed in order to visualize the relatively weak higher angle data. The diffraction orders that were observed are labelled in each pattern. The slit height used to densitometer these patterns is indicated.

width at half-maximum for the lamellar reflections of extracted lipids is nearly constant over the range of reciprocal space for which diffraction was observed, increasing by less than a factor of 1.2 from $I(h = 1)$ to $I(h = 4)$. In contrast, the full width at half-maximum increased by a factor of 2 from $I(h = 1)$ to $I(h = 4)$ for the diffraction from sarcolemmal membranes. This increase in the widths of the lamellar reflections for the sarcolemmal membrane as a function of the reciprocal space coordinate is probably indicative of lattice disorder, as observed for the sarcoplasmic reticulum [11], arising from the imperfect packing of the sarcolemmal vesicles within the multilayer. Aging of the sarcolemmal membrane multilayer sample or extensive humidity fluctuations resulted in diffraction patterns that characteristically have two sets of lamellar reflections indexing on slightly different repeat periods. For such cases, one set of reflections is qualitatively similar to that from extracted lipids while the other resembles that from sarcolemmal membrane multilayers with one set of lamellar reflections. Since the diffraction patterns from sarcolemmal membrane multilayers used for analysis were composed of a single set of

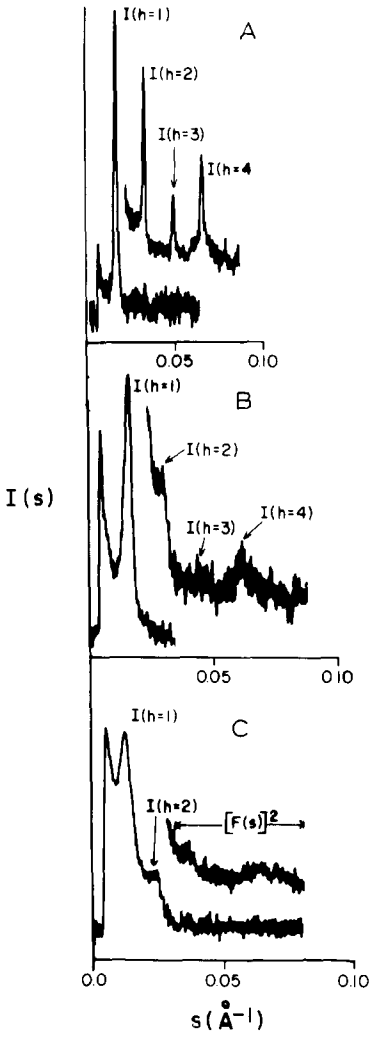

Fig. 5. Microdensitometer traces of some of the diffraction patterns shown in Fig. 4. (5A, B, C correspond to 4A, C, D, respectively). Sarcolemmal lipids (A) and the sarcolemmal membrane (B, $d = 63$ Å) patterns contain four diffraction orders. In (C), the sarcolemmal membrane pattern for $d = 77$ Å, indicates that for $I(s)$ where $s > 0.03$ Å^{-1}, the diffraction is characteristic of the unsampled structure-factor function squared, $(F(s))^2$, i.e., the interference function is near unity for this region of reciprocal space.

lamellar reflections over a broad range of repeat periods, and given the characteristics of the diffraction patterns described above, it is unlikely that the sarcolemmal membranes in the packed pellet contain phase-separated lipid. In addition, these multilayers apparently do not contain protein phase segregation as evidenced by the freeze-fracture results in the multilayer. Therefore, the sarcolemmal membrane multilayers used for diffraction studies must be intact.

An example of a background-corrected diffraction pattern for sarcolemmal membrane multilayers with $d = 63$ Å is shown in Fig. 6. The diffraction pattern (Fig. 4A) for extracted sarcolemmal lipids, $d = 60$ Å and its corresponding trace (Fig. 5A) contained four diffraction orders ($I(h = 1) \rightarrow I(h = 4)$). The diffraction pattern (Fig. 4C) for sarcolemmal membrane multilayers with $d = 63$ Å and its corresponding trace (Fig. 5B) likewise contained four diffraction orders. The diffraction pattern (Fig. 4D) from sarcolemmal membrane multilayers with $d = 77$ Å and its corresponding trace (Fig. 5C) contained only two sampled diffraction orders ($I(h = 1,2)$) along with the unsampled $[F(s)]^2$ (where $F(s)$ is the single membrane transform) for $s > 0.03$ Å^{-1}. Patterns similar to that shown in Figs. 4D and 5C were generally obtained for sarcolemmal membrane multilayers where $d > 68$ Å, and were not used in a swelling analysis.

The unit cell repeats of approx. 55–65 Å must contain a single sarcolemmal membrane when compared to the membrane widths observed in electron microscope images of thin-sectioned dispersions and oriented multilayers shown in Figs. 1 and 2 (see Fig. 7). Because of the nature of the diffraction pattern for the larger repeat (Figs. 4D, 5C) when compared to the diffraction pattern of

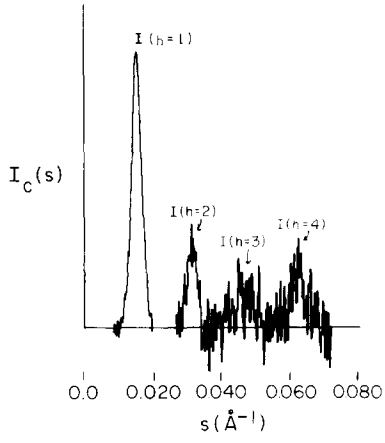

Fig. 6. Background-corrected lamellar intensity function, $I_c(s)$ corresponding to Fig. 5B, showing $I(h = 1) \rightarrow I(h = 4)$.

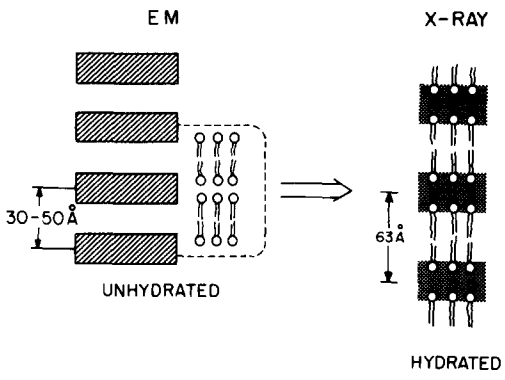

Fig. 7. Schematic picture depicting the thin-section electron microscope (EM) image of unhydrated sarcolemmal membrane multilayers with a repeat of 30–40 Å (50–70 Å in thin-section dispersions) and the unit cell repeat of 63 Å for hydrated sarcolemmal membrane multilayers, the latter obtained by X-ray diffraction (from Fig. 5B). The unit cell repeat of 63 Å is shown to contain one symmetric sarcolemmal membrane (see text).

Fig. 4B, 4C and 5B, the former represents a highly swollen state of the sarcolemmal membrane and thus the unit cell repeat also must contain a single membrane. Lipids extracted from these sarcolemmal membranes had an average multilayer unit cell repeat typical of a pure lipid bilayer structure. The mosaic spread of the lamellar reflections for the oriented pure lipid multilayer was less than that obtained for sarcolemmal membrane multilayers at a similar d spacing based on a qualitative inspection of the diffraction patterns in Fig. 4, and the reflection widths and the ratio of diffraction orders were different for intact sarcolemmal membranes and extracted lipids at a comparable d spacing (Fig. 5). These differences in the diffraction patterns for intact sarcolemma and extracted sarcolemmal lipids at a similar d spacing probably arise from small differences in stacking and lattice disorders which could reflect the presence of protein in the intact sarcolemmal membrane in contrast to the lipid extract.

A swelling analysis was performed in order to unambiguously assign phase factors to the experimentally obtained structure factors. In Table I, two sets of structure factors for different lamellar repeats ($d = 63$ and 68 Å) of the same sarcolemmal membrane multilayer are given, arbitrarily normalized to the sum of the structure factors for

TABLE I

Structure factors			
$d = 63$ Å		$d = 68$ Å	
(h)	$F(h)$	(h)	$F(h)$
1	67.1	1	64.9
2	11.6	2	23.0
3	9.4	3	12.1
4	11.9	4	0

Hierarchy of phase assignments		
$d = 63$ Å	$d = 68$ Å	Δ
$\pi\pi 0\pi$	$\pi\pi 0\pi$	0.2268
$\pi 0\pi 0$	$\pi 0\pi\pi$	0.2813
$\pi\pi\pi 0$	$\pi\pi\pi\pi$	0.3130
$\pi\pi 00$	$\pi\pi 0\pi$	0.3455
$\pi 000$	$\pi 000$	0.4152

that particular data set. The algorithm devised by Stamatoff and Krimm [30] was used to compute the Δ value for all possible phase combinations and the five most probable phase combinations ranked by their appropriate Δ values are given in Table I. This algorithm provides a hierarchy of more probable phase combinations and hence unit cell profiles, with the most probable profile possessing the least deviation (smallest Δ) with variations in multilayer repeats [15]. The phase combination, $\pi\pi 0\pi$, was obtained for this data pair as well as that for unit cell repeats equal to 56 and 63 Å (data not shown). The lipid extract data was likewise phase by this procedure and the phase factors $\pi\pi 0\pi$ were assigned. Electron density profiles on a relative electron density scale, based on this analysis of the diffraction patterns of Fig. 4A and C, at 15 Å resolution, are shown in Fig. 8 and found to be consistent with a unit cell of approx. 60 Å that contained a single symmetric membrane.

The profile structures for both purified lipids (Fig. 8A) and sarcolemmal (Fig. 8B) membranes are symmetric at this resolution and are qualitatively similar in appearence. However, the ratio of the relative electron density levels of the phospholipid headgroup to the fatty acyl chain density, a, and the fatty acyl chain density to terminal methyl trough, b, was 1.48 ± 0.06 (mean $\pm$ S.D.) for extracted lipids and 1.85 ± 0.15 for the intact membrane. The errors in these ratios were com-

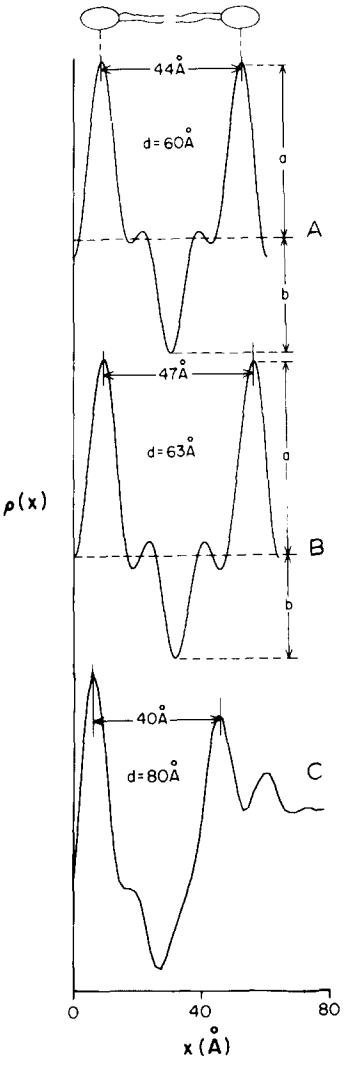

Fig. 8. Electron density profile structures of extracted sarcolemmal lipids, $d = 60$ Å (A) and the intact sarcolemmal membrane, $d = 63$ Å (B) at 15 Å resolution. The unit cell is seen to contain a single symmetric membrane with an average separation of 44 and 47 Å between the phospholipid headgroups for lipids and the intact membrane, respectively. Small differences in the electron density levels between these profile structures, as given by the ratio (a/b), is probably due to the presence of protein in the intact sarcolemmal membrane (see text). In (C), we provide the electron density profile structure of a single skeletal sarcoplasmic reticulum membrane taken from Herbette et al. [11]. The unit cell of $d = 160$ Å in this case contains a mirror plane with two asymmetric membranes corresponding to the two apposed membranes of the flattened sarcoplasmic reticulum vesicle and we show one membrane ($d' = 80$ Å, where $d = 2d'$) of this double membrane pair (i.e., the other membrane within the unit cell is a mirror image). The hydrated sarcoplasmic reticulum membrane obtained by X-ray diffraction has been shown to range from 80–120 Å, depending on the water content of the oriented multilayer.

puted by assuming 5% (extracted lipids) and 10% (sarcolemmal membrane) random errors for the intensity values based on the estimated noise fluctuations in the appropriate intensity functions. The different correction factors (s vs. s^2) applied to the intensity functions had a small effect on these ratios which fell within the standard deviations given above. In addition to these differences in the relative electron density levels, the phospholipid headgroup separation was 44 and 47 Å for extracted lipid and sarcolemmal membranes, respectively, at a similar d spacing. The profile structure in Fig. 8C is for a single membrane of skeletal sarcoplasmic reticulum, taken from Herbette et al. [11], and is reproduced here for comparison to the sarcolemmal membrane. The profile structure for sarcoplasmic reticulum shows the greater overall membrane width and highly asymmetric nature of this membrane compared to the sarcolemmal membrane. The phospholipid headgroup separation for both the sarcoplasmic reticulum membrane and extracted sarcoplasmic reticulum lipids (data not shown) was 40 Å, considerably smaller than that for the sarcolemmal membrane [11,15].

Discussion

The skeletal sarcoplasmic reticulum membrane contains a single essential protein, the Ca^{2+} pump ATPase, which is responsible for a single well-defined function – that of calcium transport. The cardiac sarcoplasmic reticulum membrane is somewhat more complex, as the Ca^{2+} pump is regulated by both cyclic AMP- and Ca^{2+}-dependent phosphorylation [32]. In contrast, the sarcolemma utilizes several mechanisms for the transport of ions and other substances, and contains receptor sites for binding of various ligands [1,33,34], implying that the architecture of the sarcolemma is madeup of many protein components. For these reasons, cardiac sarcolemma would be expected to differ structurally from both skeletal and cardiac sarcoplasmic reticulum.

Sarcolemmal membrane width

Studies of the 'accessibility' of the $(Na^+ + K^+)$-ATPase enzyme and ouabain-binding sites in sarcolemmal vesicle preparations described in this report indicate that these preparations contained

approx. 70% sealed vesicles, of which 90% were right-side-out [1]. Thin-section electron microscopy demonstrated that these preparations contained closed, predominantly unilamellar vesicles (Fig. 1). The average width from thin-sectioned dispersions of the sarcolemmal membrane was approx. 50–70 Å, similar to that of a pure lipid bilayer. Several electron microscopy techniques failed to show substantial amounts of protein protruding from either surface of the stained 'double-track' lipid bilayer of the sarcolemmal membrane. Two plausible explanations for this observation are, (a) the various fixatives used in these electron microscopy studies might not have interacted efficiently with sarcolemmal membrane proteins and (b), since the lipid-to-protein ratio for the sarcolemmal membrane is relatively high [1] compared to other membranes such as the sarcoplasmic reticulum and the $(Na^+ + K^+)$-ATPase, the density of proteins at the surface of the sarcolemmal membrane may be too low to result in the reaction of a sufficient amount of fixative/stain that can be visualized in the electron microscope.

Analysis of thin sections of fixed oriented sarcolemmal membrane multilayers provides evidence against the first explanation, because close packing of the sarcolemmal membranes would maximize the visualization of protein protruding from either surface of the lipid bilayer. This observation is based on the finding that when dispersions of the sarcoplasmic reticulum membrane are fixed with only osmium, this membrane has the appearance of a lipid bilayer with a sparsely fixed extravesicular surface coat from which one would underestimate the true thickness of this membrane. Thin-sectioned dispersions of the sarcoplasmic reticulum fixed with tannic acid and osmium clearly define the membrane width to be approx. 100 Å, similar to that derived from X-ray diffraction studies [15]. However, when membrane multilayers of the sarcoplasmic reticulum are fixed with only osmium via the vapor phase, the average membrane width as measured in the multilayer is approx. 90 Å. Thus, these observations regarding a comparison of membrane widths as measured in thin sections of dispersions and multilayers suggest that, on average, their appears to be a negligible amount of protein that protrudes from either surface of the sarcolemmal lipid bilayer, where there is at most a 3-fold difference in the lipid-to-protein ratio between the sarcolemma and sarcoplasmic reticulum.

The thin-sectioned membrane profiles of sarcolemmal vesicles in dispersions have a symmetrical appearance which is confirmed by the observation that the 'banding pattern' found in thin sections of sarcolemmal membrane multilayers (Fig. 2) is symmetric with a regular repeat of 30–40 Å. This repeat though small is representative of the unhydrated fixed sarcolemmal membrane in a compressed multilayer and is similar to the dimensions of a lipid bilayer (see Figs. 2 and 7). Since this repeat represents the center-to-center distance for the electron dense bands in the fixed multilayer, it is expected to be less than or equal to the average membrane width as observed in fixed dehydrated dispersions and both of these widths are usually observed to be less than the width of the corresponding hydrated membrane [15]. Thin-sectioned membrane profiles of both skeletal (Fig. 1B) and cardiac (data not shown) sarcoplasmic reticulum vesicle dispersions appear highly asymmetric. Thin-sectioned multilayers of the sarcoplasmic reticulum show a highly asymmetric 'banding pattern' with a regular average repeat of 180 Å. This repeat, which is similar to the unit cell repeat obtained by X-ray diffraction, represents the two apposed asymmetric membranes of the flattened sarcoplasmic reticulum vesicle, each having a membrane width of approx. 90 Å [15]. In contrast, the sarcolemma appears as a symmetric, relatively thin membrane when observed in the electron microscope.

X-ray diffraction is a more sensitive probe of membrane fine structure than is electron microscopy and can be used to obtain an estimate of membrane width where the functional state of the membrane is preserved, since the membrane is not fixed [11]. Lamellar X-ray diffraction studies of hydrated oriented sarcolemmal membrane multilayers showed that lamellar repeat distances of 56–77 Å could be obtained, depending on the water content of the membrane multilayer. Hydrated lipids extracted from the sarcolemmal membrane had a lamellar repeat distance of 56–62 Å. Since the electron microscope studies have shown that the center-to-center repeat for a single unhydrated sarcolemmal membrane in the multi-

layer is 30–40 Å, and the width of the membrane in fixed dispersions is 50–70 Å, the repeat obtained by X-ray diffraction can be considered to represent a unit cell containing one sarcolemmal membrane with water layers between membranes as depicted in Fig. 7. This technique has limitations in that (a) the scattering is representative of the average unit cell structure within the multilayer sample and, (b) proteins that protrude from the sarcolemmal membrane lipid bilayer that are present at low densities in the membrane, may not be detected by X-ray diffraction since they may 'fold' up in the edges of the flattened vesicle as unoriented material which would scatter incoherently. Thus, these data show that the average sarcolemmal membrane width is considerably less than that of the sarcoplasmic reticulum. The average width for this sarcolemmal membrane is smaller than that reported in a review by McNutt [35] where it was suggested that the general sarcolemma was 75–90 Å thick.

Freeze-fracture interpretations

Freeze-fracture images of sarcolemmal vesicles (Fig. 3) consistently showed major particles of 80–90 Å diameter present primarily on the convex fracture surface. The distribution of large particles mainly on the convex fracture face of sarcolemmal vesicles is consistent with a single particle orientation with respect to sidedness. Measurements of vesicle sidedness suggest that the convex fracture face, which contains most of the large particles, corresponds to the inner monolayer surface of right-side-out vesicles [1]; this represents the cytoplasmic leaflet of the sarcolemma. The concave fracture face of skeletal sarcoplasmic reticulum, which corresponds to the outer monolayer surface, contains virtually all of the large particles in this intracellular membrane, and thus represents the cytoplasmic leaflet. As ATP binds at the cytosolic leaflet of both membrane systems, the origin of fracture surfaces in sarcolemmal vesicles is consistent with the freeze-fracture appearance of sarcolemma in the intact myocardial cell [36–38].

The origin of the large particles on the convex fracture surface of sarcolemmal vesicles is difficult to determine and, presently, can only be inferred from comparisons of the structural properties of the sarcoplasmic reticulum and sarcolemmal membranes. It has been shown that the $(Na^+ + K^+)$-ATPase is the major protein in these sarcolemmal preparations [1,39], so it is tempting to conclude that the freeze-fracture particles observed for sarcolemmal vesicles arise from this protein. It is interesting that the size of the freeze-fracture particles on the convex fracture surface of sarcolemmal vesicles (80–90 Å) is similar to that observed for the freeze-fracture particles on the concave fracture surface of the sarcoplasmic reticulum (75–80 Å). For both membrane systems, these particles appear to protrude significantly above the freeze-fracture plane. Napolitano et al. [14] have previously compared the unit cell area occupied by each freeze-fracture particle and its associated lipid matrix in the sarcoplasmic reticulum with the average cross-sectional area occupied by the monomeric calcium pump protein and its associated lipid obtained separately by X-ray and neutron diffraction methods. This comparison of the unit cell areas obtained from two independent techniques suggested that each freeze-fracture particle probably represents a dimer of pump protein molecules in the plane of the sarcoplasmic reticulum membrane. Although the monomeric/oligomeric nature of the calcium pump protein is still highly debated, the dimer model is also supported by recent freeze-fracture studies of reconstituted sarcoplasmic reticulum [40] and kinetic data for calcium transport [41]. Since the $(Na^+ + K^+)$-ATPase and calcium pump protein have comparable monomeric molecular weights [39] and molecular lengths [11,13,14,16,42], the monomeric form of these proteins must have similar molecular volumes and hence average cross-sectional areas. Since the average cross-sectional area of freeze-fracture particles for sarcolemma (approx. 5700 $Å^2$) is similar to that for sarcoplasmic reticulum (approx. 4700 $Å^2$) and each freeze-fracture particle seen in the sarcoplasmic reticulum membrane probably represents a calcium pump protein dimer [14,40,41], it is conceivable that the large freeze-fracture particles observed for sarcolemmal membranes might represent a $(Na^+ + K^+)$-ATPase dimer. This argument is somewhat weakened by the observation that the estimated ouabain-binding site density for sarcolemmal membranes (330 μm^{-2}) [1] was half the density of large particles in freeze fracture (780 ± 190 μm^{-2}). This dis-

crepancy is not explained, but the greater particle density observed by freeze fracture may be due to other proteins of molecular weight comparable to the $(Na^+ + K^+)$-ATPase as observed for these preparations [1,43].

The particle density for freeze-fracture surfaces of intact cardiac sarcolemma [36–38] with its associated or partially associated glycocalyx (2000–2600 particles/μm^2) is greater than that for sarcolemmal vesicles, in which the glycocalyx is completely removed. The lower particle density in our sarcolemmal membrane fraction may thus be related to loss of peripheral and integral membrane proteins during preparation of sarcolemmal vesicles. An alternative argument may reflect differences in the freeze-fracture method. The particle density range of 2000–2600 μm^{-2} observed by Frank et al. [36–38] was obtained from rotary-shadowed replicas and was independent of calcium concentration (i.e., zero calcium vs. controls). They report that particle densities for unidirectionally shadowed replicas in zero calicum (800–1000 μm^{-2}) appeared lower than controls (2200 μm^{-2}). Since our preparations are prepared in the absence of calcium and are unidirectionally shadowed, our values are consistent with those of Frank et al. [36–38] using similar techniques and this may represent an inadequacy of the technique to detect protein particles in zero or low calcium. In addition, it is difficult to make definitive comparisons of particle densities obtained from intact tissue [35–38,44] and sarcolemmal fractions since the glycocalyx surface coat may contribute particles found in the sarcolemma.

The packing density of particles in skeletal sarcoplasmic reticulum is approx. $11\,500 \pm 2000$ μm^{-2} [14], in contrast to both our much lower density of 780 ± 190 μm^{-2} for sarcolemma or the 2000–2600 μm^{-2} density observed in the intact myocardial cell [36–38]. The significantly higher lipid/protein ratio of the sarcolemma than sarcoplasmic reticulum and the difference in protein composition of the sarcoplasmic reticulum and the sarcolemmal membranes both appear to contribute to this difference. The greater lipid content of sarcolemma compared to sarcoplasmic reticulum results in a greater area of the sarcolemmal membrane surface occupied by lipid and hence a lower particle density. Furthermore, the sarcoplasmic reticulum membrane contains mainly the 119000 dalton calcium pump ATPase protein that makes up these particles, whereas the sarcolemmal membrane has a heterogeneous protein profile [1]. The sarcolemmal proteins in the 90000–150000 dalton range are large enough to contribute particles to the freeze-fracture surfaces, but the many low molecular weight proteins in the sarcolemmal membrane may not be detectable by this technique.

Interpretations of sarcolemmal membrane profile structure

At the resolution obtained in these studies, the electron density profile of the sarcolemmal membrane represents a single symmetric membrane bilayer similar to that of extracted sarcolemmal lipids (Fig. 8A and B). The electron dense maxima within the profile structure of the intact sarcolemmal membrane and extracted lipids represent phospholipid headgroups; the central trough represents the terminal methyl group region of the bilayer; between these extremes lie the fatty acyl chains of the lipid bilayer hydrocarbon core. The overall similarity in the profile structures for sarcolemma and extracted lipids is in accord with the very high lipid content of the sarcolemmal membrane [1].

A close examination of the sarcolemmal membrane and extracted lipid profile structures (Fig. 8) shows that the phospholipid headgroup separation in the sarcolemmal membrane is slightly greater (47 Å) than that for extracted lipids (44 Å), although this can be accounted for by the slight difference in their unit cell dimensions. Comparison of the profile structures of the sarcolemmal membrane with extracted lipids at the same unit cell dimension, $d = 56$ Å, showed that the headgroup separation was the same to within 1 Å (data not shown). Thus, the thickness of the hydrocarbon core is the same whether or not sarcolemmal proteins are present. In addition, fine perturbations of the electron density levels within the sarcolemmal membrane profile were seen when compared to the electron density levels within the profile structure of extracted sarcolemmal lipids. Since placement of these profile structures on an absolute electron density scale is difficult, the relative electron density levels were compared. The

level of the headgroup density to the fatty acyl chain density (a) was compared to the level of the fatty acyl chain density to the terminal methyl hydrocarbon core density (b). This ratio (a/b) was equal to 1.48 for the profile structure of extracted lipids and 1.85 for the intact sarcolemmal membrane. Since the phospholipid headgroup density is usually approximately 0.43 $e/Å^3$, the water density is 0.334 $e/Å^2$ and the average protein density is usually 0.4 ± 0.1 $e/Å^3$ [17,28], the headgroup density can only be decreased by addition of protein or water to this region of the profile structure. In contrast, the fatty acyl chain region and terminal methyl region usually have densities of 0.28 and 0.23 $e/Å^3$ [15,28], respectively, and so would be increased if protein were added to this region. The greater ratio (a/b) for the intact sarcolemmal membrane profile structure than the profile structure of extracted lipids indicates that the density within the hydrocarbon core may be higher for the intact sarcolemmal membrane compared to that for extracted lipid. These findings therefore suggest the presence of protein either within the central hydrocarbon core region of the sarcolemmal membrane, or completely spanning the membrane, uniformly distributed between both monolayers of the sarcolemmal membrane bilayer, or both. Thus, low concentrations of these proteins (i.e., high lipid/protein ratio) can also explain the small perturbations in the lipid bilayer structure of the intact membrane and the symmetrical appearance of the profile structure at the resolution obtained.

Comparison of the profile structures for the sarcolemmal and sarcoplasmic reticulum membranes shows significant differences consistent with the large differences in their lipid-to-protein ratios [1]. The contribution of protein to the sarcoplasmic reticulum profile structure is evident in the asymmetry of the hydrocarbon core region and the 'protein knob' external to the sarcoplasmic reticulum lipid bilayer. The separation of the phospholipid headgroups in the sarcolemmal membrane is significantly greater than that observed in the sarcoplasmic reticulum membrane (Fig. 8C) and lipids extracted from the sarcoplasmic reticulum membrane (Refs. 11, 15, and data not shown), the latter being 40 Å. Thus, the hydrocarbon core of the sarcolemmal membrane bilayer is approx. 18% thicker than that of the sarcoplasmic reticulum. This difference in hydrocarbon core width may be due to either the different fatty acyl chain composition of these two membranes or the presence of small proteins contained within the hydrocarbon core of the sarcolemmal membrane bilayer. The latter interpretation may be correct based on a comparison of the profile structures of the intact sarcolemmal membrane and lipids extracted from this membrane (see Discussion above). Furthermore, purified $(Na^+ + K^+)$-ATPase membranes have a thickness (80–100 Å) similar to that of the purified skeletal sarcoplasmic reticulum membrane [42]. The relatively low concentration of the $(Na^+ + K^+)$-ATPase and other proteins in the sarcolemmal membrane [1] probably explains our inability to detect a significant contribution of protein to the total scattering profile; a higher concentration of the $(Na^+ + K^+)$-ATPase would have been expected to result in a greater average membrane width for the sarcolemma.

Implications of sarcolemmal membrane structure

The structure of the sarcoplasmic reticulum membrane is much different from that of the sarcolemma. Although the sarcoplasmic reticulum membrane from cardiac muscle is more complex than that from skeletal muscle, the essential structural-functional features of both of these membranes reflect the predominance of the calcium ATPase protein. The relatively high lipid-to-protein ratio of the sarcolemma [1], may be important in the conduction of the cardiac action potential. The high lipid content of the sarcolemma may also serve as an efficient barrier to the transfer of important physiological ions, e.g., calcium [45]. Finally, this high content of lipid may also provide an efficient mechanism that allows for lipid-soluble transmitters, hormones and drugs to interact with protein receptors by first partitioning into the membrane bilayer and then laterally diffusing to their respective receptor sites contained within this membrane bilayer.

Acknowledgements

The authors wish to thank Dr. J. Watras for supplying cardiac sarcoplasmic reticulum to us, Dr. G. Sarmiento for helpful discussions regarding

various aspects of receptor biochemistry with the sarcolemma, and Dr. A.M. Katz for helpful discussions regarding this manuscript. This work was supported by NIH grants HL-32588, HL-27630, HL-21812, HL-22135 and HL-26903, by a grant from the American Heart Association and by a University of Connecticut Research Foundation grant. R.A.C. was a postdoctoral fellow supported by NIH grant HL-07420. L.G.H. is a Charles E. Culpeper Foundation Fellow.

References

1 Colvin, R.A., Ashavaid, T.F. and Herbette, L. (1985) Biochim. Biophys. Acta 812, 601–608
2 Jones, L.R., Madlock, S.W. and Besch, H.R. (1980) J. Biol. Chem. 255, 9971–9980
3 Hasselbach, W. and Makinose, M. (1961) Biochem. Z. 333, 518–528
4 Ebashi, S. and Lipmann, F.J. (1962) J. Cell Biol. 14, 389–400
5 Tada, M., Yamamoto, T. and Tonomura, Y. (1978) Physiol. Rev. 58, 1–79
6 Baskin, R.J. and Deamer, D.W. (1969) J. Cell Biol. 42, 296–307
7 Dupont, Y., Harrison, S.C. and Hasselbach, W. (1973) Nature (Lond.) 244, 555–558
8 Worthington, C.R. and Liu, S.C. (1973) Arch. Biochem. Biophys. 157, 573–579
9 Tillack, T.M., Boland, R. and Martonsi, A. (1974) J. Biol. Chem. 249, 624–633
10 Davis, D.G, Inesi, G. and Gulik-Krzywicki, T. (1976) Biochemistry 15, 1271–1276
11 Herbette, L., Marquardt, J., Scarpa, A. and Blasie, J.K. (1977) Biophys. J. 20, 245–272
12 Herbette, L. (1980) Ph.D. Dissertation, University of Pennsylvania, Philadelphia
13 Blasie, J.K., Pachence, J.M. and Herbette, L. (1983) in Neutrons in Biology (Schoenborn, ed.), Brookhaven Symposium, Plenum Press, New York, 27, 201–210
14 Napolitano, C.A., Cooke, P., Segalman, K. and Herbette, L. (1983) Biophys. J. 42, 119–125
15 Herbette, L., Scarpa, A., Blasie, J.K., Wang, C.T., Saito, A. and Fleischer, S. (1981) Biophys. J. 36, 47–72
16 Blasie, J.K., Herbette, L., Pierce, D., Pascolini, D., Scarpa, A. and Fleischer, S. (1983) Ann. NY Acad. Sci. 402, 478–484
17 Herbette, L., Scarpa, A., Blasie, J.K., Wang, C.T., Hymel, L., Seelig, J. and Fleischer, S. (1983) Biochim. Biophys. Acta 730, 369–378
18 Brady, G.W., Fein, D.B., Harder, M.E. and Meissner, G. (1982) Biophys. J. 37, 637–645
19 LeMaire, M., Moller, J.V. and Tardieu, A. (1981) J. Mol. Biol. 150, 273–296
20 Dux, L. and Martonosi, A. (1983) J. Biol. Chem. 258, 2599–2603
21 Katz, A.M. and Repke, D.I. (1967) Circ. Res. 21, 153–162
22 Katz, A.M., Repke, D.I. and Hasselbach, W. (1977) J. Biol. Chem. 252, 1938–1949
23 Rathier, M., Watras, J. and Katz, A.M. (1982) Fed. Proc. 41, 1524a
24 Watras, J., Messineo, F. and Herbette, L. (1984) J. Biol. Chem. 259, 1319–1324
25 Lowry, O., Rosebrough, N., Farr, A.L. and Randall, R. (1951) J. Biol. Chem. 193, 265–275
26 Conte, S.D. and DeBook, C. (1972) Elementary Numerical Analysis, pp. 233–240, McGraw-Hill, New York
27 Pachence, J.M., Dutton, P.L. and Blasie, J.K. (1981) Biochim. Biophys. Acta 635, 267–283
28 Pachence, J.M., Dutton, P.L. and Blasie, J.K. (1979) Biochim. Biophys. Acta 548, 348–373
29 Moody, M.F. (1963) Science 142, 1173–1174
30 Stamatoff, J.B. and Krimm, S. (1976) Biophys. J. 16, 503–516
31 Guinier, A. (1963) X-Ray Diffraction, W.H. Freeman, San Francisco
32 Tada, M. and Katz, A.M. (1982) Annu. Rev. Physiol. 44, 401–423
33 Deplover, A., Matlib, M.A., Lee, S.W., Bube, G.P., Grupp, I.L., Grupp, G. and Swartz, A. (1982) Biochem. Biophys. Res. Commun. 108, 110–117
34 Sarmiento, J.G., Janis, R.A., Colvin, R.A., Triggle, D.J. and Katz, A.M. (1982) J. Mol. Cell. Cardiol. 15, 135–138
35 McNutt, N.S. (1975) Circ. Res. 37, 1–13
36 Frank, J.S., Langer, G.A., Nudd, L.M. and Seraydarian, K. (1977) Circ. Res. 41, 702–714
37 Frank, J.S., Beydler, S., Kreman, M. and Rau, E.E. (1980) Circ. Res. 47, 131–143
38 Frank, J.S., Rich, T.L., Beydler, S. and Kreman, M. (1982) Circ. Res. 51, 117–130
39 Jørgensen, P.L. (1982) Biochim. Biophys. Acta 694, 27–68
40 Wang, C.T., Saito, A. and Fleischer, S. (1979) J. Biol. Chem. 254, 9209–9219
41 Ikemoto, N., Garcia, A.M., Kurobe, Y. and Scott, T.L. (1981) J. Biol. Chem. 256, 8593–8601
42 Deguchi, N., Jørgensen, P.L. and Maunsbach, A.B. (1977) J. Cell Biol. 75, 619–634
43 Jones, L.R., Besch, H.R., Fleming, J.W., McConnaughey, M.M. and Watanabe, A.M. (1979) J. Biol. Chem. 254, 530–539
44 Ashraf, M. (1979) Am. J. Pathol. 97, 411–432
45 Urry, D.W., Trapane, T.L., Walker, J.T. and Prasad, K.U. (1982) J. Biol. Chem. 257, 6659–6661